Executive Summary for ESA Contract No. 4000134266/21/NL/GLC/ov

Sub nano-g MEMS accelerometer for high precision orbital manoeuvres

Version 1.7

FINAL

PUBLIC

1 Introduction

The goal of this project is to accelerate the development and (aero)space market entry of a next generation of inertial sensing. Ultimately, through the commercialisation of this technology and the improved capabilities and business models of its users, the consortium hopes to usher in the next era of key space infrastructures and endeavours.

In the pursuit of advanced gravitational wave detection, Nikhef, the Dutch National Institute for Subatomic Physics, started developing a novel seismic sensor: An ultra-sensitive miniaturised accelerometer made in micro-electro- mechanical system (MEMS) technology, as shown in Figure 1. The goal was to develop an affordable accelerometer that was as sensitive as conventional seismometers, but significantly smaller and cheaper. Innoseis, a spin-off company, has been licensed to bring this cutting-edge technology to market.

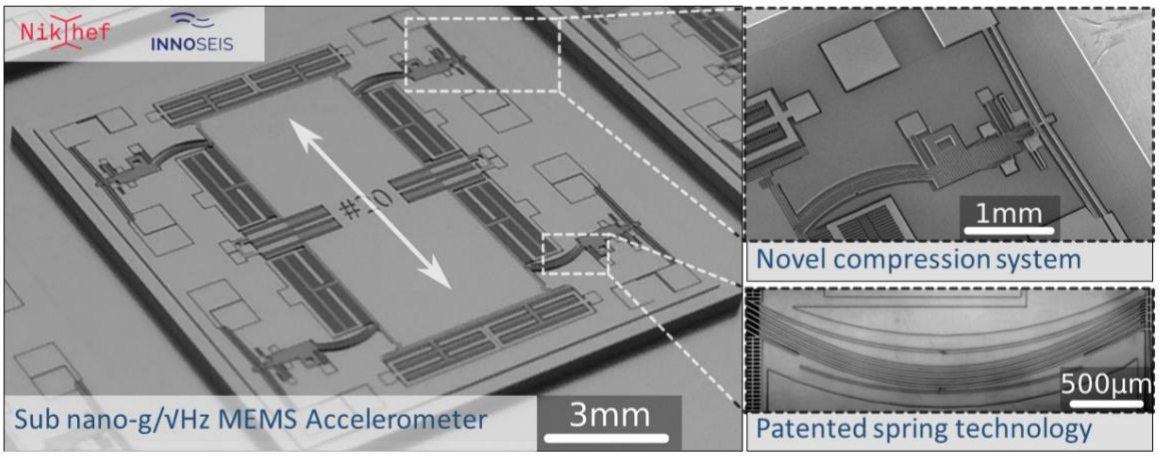

Figure 1: Example of a prototype MEMS accelerometer with patented anti-spring technology

The high-sensitivity MEMS accelerometer is a breakthrough innovation. It is a significant improvement on the existing state-of-art. In terms of key performance metrics, the sensors offer a 100 fold improvement in sensitivity and stability while achieving a 10 times energy reduction.

2 Aerospace application

The MEMS sensors are expected to be sold into the broader high-end inertial sensor market, of which commercial aerospace is an important segment. In 2019 the high-end inertial sensor market was reported to be worth $3.24B, of which commercial aerospace made-up 25% ($ 800M) behind Defence and Military (40%) and ahead of Commercial Naval (18%) and Industrial (17%), with the aerospace segment expected to grow with a CAGR of 4.5% until 2025. (source: High-End Inertial Sensors for Def. Aero. Ind. Apps Rep. 2020, Yole Dev. 2020).

Use cases within the aerospace industry exist in which a step change improvement in sensor performance could have a significant impact. The exploration of these use cases and an analysis of the anticipated impact is a topic of this project. A broad range of potential use cases are discussed, and a short list was selected being considered to have the most commercial and technical potential:

- Precision orbit determination for (constellations of) satellites is seen as an attractive application area due to the technological fit in combination with higher volumes. Improved orbit determination will allow for more accurate and autonomous positioning. With higher

volumes the cost price will be able to be driven down further allowing for a competitive advantage in this and other applications

- Deep Space missions and the precision inertial navigation of space craft over longer periods of time are also seen to have a good technologic fit. This product will provide a solution that is currently unfulfilled yet desirable for such use cases.
- Another set of application areas have been identified that could utilize the same collection of sensors while solving various challenges: Flexible mode / sloshing, FDIR monitoring, and Delta-V monitoring all have a good qualitative overlap with the key performance indicators. Synergy could be found in the use of multiple sensor units throughout the craft to perform the required monitoring and analysis.

This report also highlights a number of use cases discussed with potential end users which would clearly benefit from the step change improvements offered by the MEMS accelerometers.

3 Target specifications and testing plan

A list of specifications was defined, and a test plan designed to validate most of the performance characteristics. Here we present a list of only the key performance metrics.

Parameter	Description	Target	Unit
Input range	Largest detectable motion	0.2 / 2	g
Bias:			
Stability	Stability of measurements over an extended time (at constant temperature)	< 0.1	µg (1 hr)
Thermal sensitivity residual	Residual after (polynomial) compensation of systematic effect	< 10	µg
Scale factor:			
Error	Due to non-linearity / asymmetry	< 80	ppm
Thermal sensitivity residual	Residual after (polynomial) compensation of systematic effect	<100	ppm
Bandwidth	Measurement output frequency range -3 dB point magnitude	0 – 100 / 200	Hz
Noise:			
For ± 0.1 g input range: Noise level In-band noise		10 42 ng_{rms} (0-10 Hz) 95 ng_{rms} (10-100 Hz)	ng/√Hz
For ± 2 g input range: Noise level In-band noise		40 170 ng_{rms} (0-10 Hz) 400 ng_{rms} (10-200 Hz)	ng/√Hz

4 Simulation of performance for space applications

A campaign of simulations set out to determine the relative impact of the various error terms effecting the accelerometer and of the performance in a test case example. The chosen test case was the direct measurement of a low thrust and long duration manoeuvres on a spacecraft in geostationary orbit: The 70 mN thrusters on a 1000 kg satellite were engaged for 25 minutes at a time, producing a simulated continuous acceleration of 7 µg. The accelerometer error terms analysed were:

- Bias random walk (BRW),
- Bias instability (flicker noise),
- Velocity random walk (VRW, or white noise),
- Mechanical noise,
- Bias residual, and
- Scale factor error.

Two approaches were taken in the error term evaluation: an analytical analysis, including a covariance propagation method, and a numerical approach with a Monte Carlo analysis. The analytical analysis offers a relatively straight forward insight into the contributions of some of the accelerometer error terms. It is shown that from the modelled disturbances the largest contribution to the error budget is from the bias random walk.

The Monte Carlo analysis is a useful tool for comparison with analytical models and to expand the simulations to include additional noise contributions such as bias residual and instability. Comparable results are found for the analytical and Monte Carlo approaches for the bias, velocity, and scale factor random walk disturbances. The largest error term after bias compensation, was again the bias random walk. An example of the velocity error, or delta-V, during a 25-minute thrust manoeuvre from 100 Monte Carlo runs is shown in Figure 2. From these findings it can also be concluded that in the further development of the accelerometer and its read-out electronics particular care should be taken to reduce bias residual and bias random walk, while the requirements could be relaxed on factors that influence velocity random walk and scale factor error.

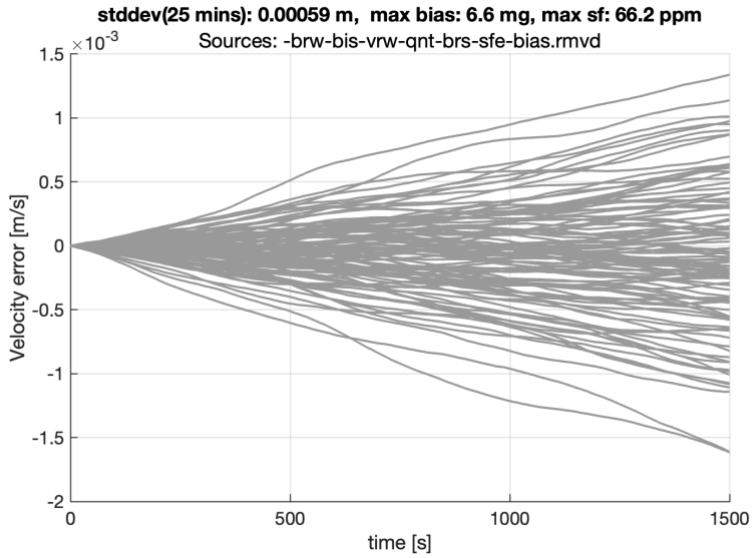

Figure 2: Monte Carlo simulation with all error terms and application of bias residual removal

Accounting with all noise terms the delta-V is shown to be less than 1%. In terms of orbit keeping for geostationary spacecraft, the 1σ delta-V error after a thrust manoeuvre is 5.9 x 10^{-4} m/s. Such spacecraft, using low thrust propulsion, typically make manoeuvres every second day to stay within its slot of 150 km on the geostationary arc. The typical yearly delta V for east west manoeuvres is 3-4 m/s or only 2 cm/s per day that a manoeuvre is executed. Considering this, the accuracy of the accelerometer during the simulated manoeuvre is sufficiently accurate, to achieve autonomous navigation for orbit keeping.

5 Design and build

With target specifications and a testing plan completed, a new readout electronics platform was designed. With respect to previous generation read-out electronics this included the following changes and improvements:

- Board level temperature measurements with temperature sensor situated as close to the MEMS as possible
- Local flash memory storage capability to store MEMS and auxiliary sensor data over extended periods of time
- Extension to allow for external timing, either via an external clock or an onboard GPS receiver
- More powerful (yet still low power consumption) FPGA to facility more complex feedback and control algorithms
- High speed interfacing over a USB interface to extract real time or recorded data

A high-level schematic of the read-out electronics is given in Figure 3. In parallel, yet out of the scope of this project the MEMS devices themselves were also prepared and tested (see Figure 4 left) and then vacuum packaged by a third party (SAES Getters). Activities also included the design and manufacture of testing equipment required to complete the testing plan. For example, a MEMS electronics board platform that can hold three MEMS boards at the same orientation, and a rotation platform that can be controlled remotely (see Figure 4 right).

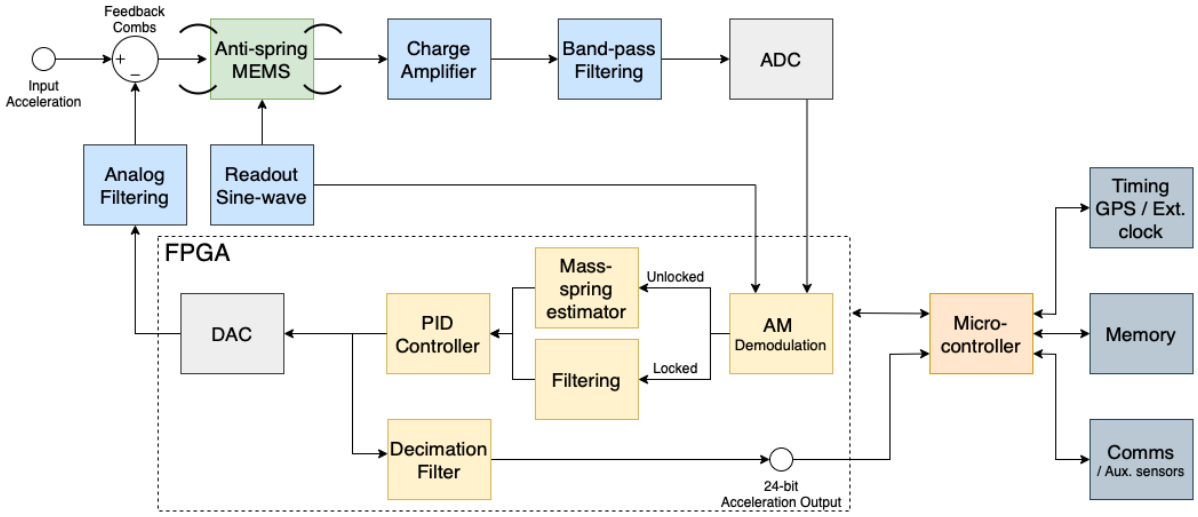

Figure 3: Schematic of read-out electronics

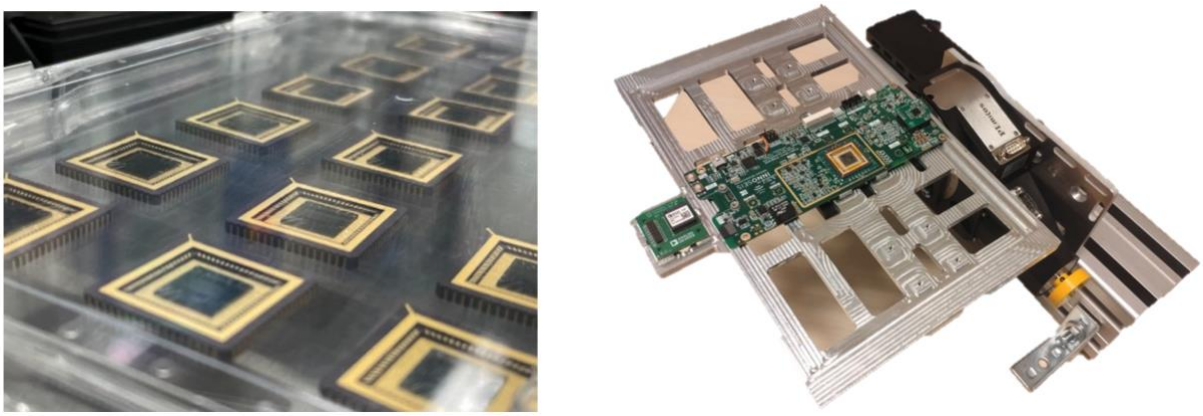

Figure 4: Left) MEMS devices bonded, tested and ready for vacuum packaging. Right) Rotation platform with a single MEMS board mounted together with a reference sensor. There are two more locations for MEMS boards.

6 Testing and validation

Preliminary testing started with a comparison between the MEMS accelerometer output and that of a reference geophone sensor. Good coincidence between the sensors is shown between 0.15 and 20 Hz. Consider the challenge of measuring the noise of a highly sensitive accelerometer – everywhere you put it, it measures something. It is therefore needed to use specialized vibration isolation facilities or environments with low(er) background vibration. The devices were installed at 'Heimansgroeve', the underground seismic observatory of the Royal Netherlands Meteorological Institute (KNMI). Within the Netherlands this is known to be the most seismically quiet location.

The power spectral density of the MEMS data from a 48-hour period at the Heimansgroeve is shown in Figure 5. The data from a reference Trillium 120s seismometer is also shown. It was evident that seismic background noise at this location in lower than at our offices in Amsterdam, however, not low enough to directly measure the MEMS noise across the full bandwidth. Using correlation analysis it was possible to extract the noise from the data (blue curve in Figure 5). The velocity random walk (white noise) is roughly 20 ng/√Hz. This is below the upper variant target of the specifications. Also, the bias random walk and bias instability (flicker noise) are seen to be below this specification down to 10 mHz.

To understand the bias stability performance an Allan variance plot is typically used. It is a measure of the stability of the acceleration measurement over varying time intervals, τ. It is shown in Figure 6 when derived from the noise measurements. Here the target stability of 0.1 μg is also plotted and it is evident that this criterion is achieved for all but the longer time intervals, depending on the device and the measurement period.

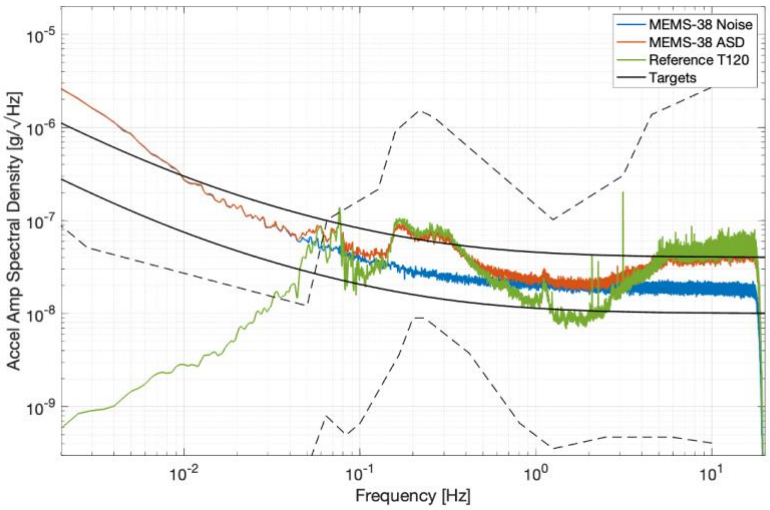

Figure 5: Amplitude power spectral density of from 24 hours of continuous data. The red curve is the MEMS sensor, the green curve the Trillium 120s reference seismometer. The target sensitivities are plotted as the solid and dashed black curve, representing variants of the accelerometer. The thin dashed black lines indicate the Peterson new high and low noise models.

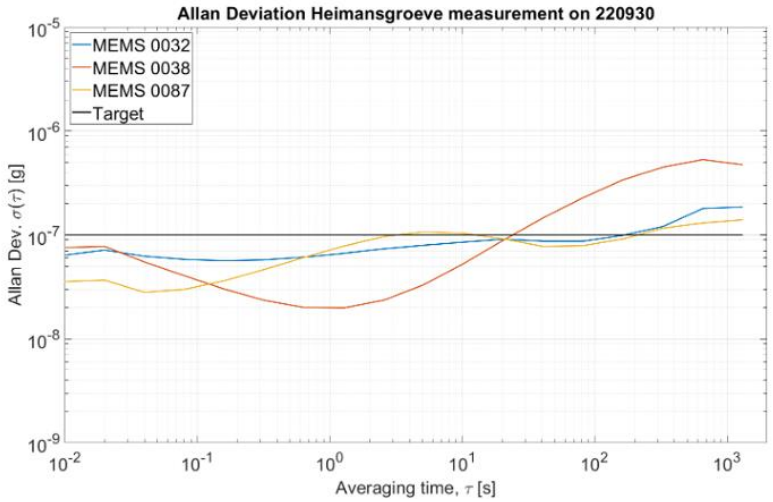

Figure 6: Alan variance of the MEMS accelerometers at the Heimansgroeve measurements. The target of 0.1 μg is indicated (black curve)

Several preliminary measurements were performed to investigate the temperature dependence of the accelerometer bias. Measuring below room temperature proved extra challenging due to the amount of vibrations created by the compressors and ventilation. Good data was however gathered in the temperature range between $20\,°C$ and $65\,°C$. Figure 7 shows two thermal cycles of the same MEMS devic. There is a clear temperature dependence and an approximate temperature sensitivity of 37 $\mu g/K$. After subtracting this third order fit from the measured data, we estimate the residual error. From this error data, we can calculate a 1σ deviation which was found to be roughly 50 µg. Further testing will be done to determine the temperature compensation and residual performance over the full temperature range and multiple devices.

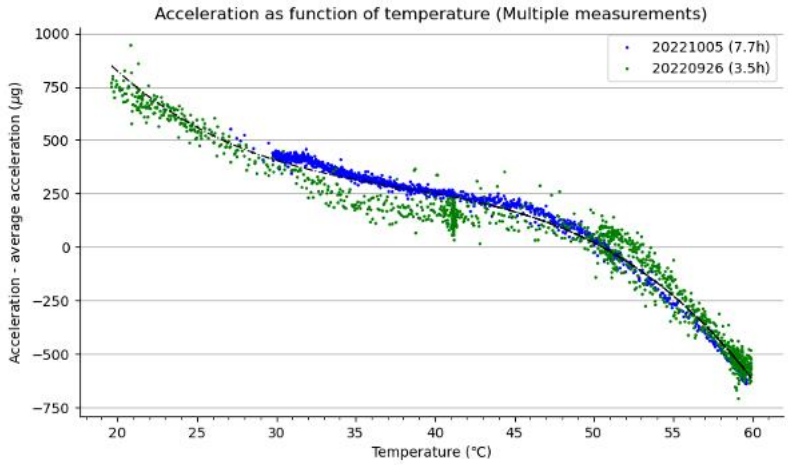

Figure 7: The measured acceleration plotted as a function of temperature, of two cycles combined. A third order polynomial fit is shown with a dashed line.

7 Design for space

From discussions with potential users, we have discovered several specific requirements for use in space applications. For example, interfacing with the rest of the spacecraft, timing synchronization and enclosure design. All these considerations come with a set of trade-offs in terms of performance, power consumption, and cost. Understanding these trade-offs to make correctly informed decisions on continuing development will be the topic of future activities. A preliminary design for a three-component unit is presented (see Figure 8). A development plan towards space qualified devices outlines how the continued testing of the sensor's critical functions in a relevant environment will bring the technology to TRL 5. With the subsequent design, manufacturing and testing of an engineering model the development will reach TRL 6.

Figure 8: Conceptual design of a three-component accelerometer unit for use in space applications

8 Conclusion and discussion

The project has been an extremely valuable steppingstone towards the application in space for our next generation acceleration sensors. Much knowledge was gained by the participates through the interaction with ESA, as well as in cooperating with each other to the meet the project objectives. A foundation has been laid for a continuation of the sensor development that will ultimately benefit a broad range of vendors and institutes, who will have access to acceleration sensing at an unprecedented level. Initial discussions with end-users, prompted by the project goals, have proven that actual and relevant uses-cases exist for the application of ultra-high sensitivity and stability accelerometers. Furthermore, results of simulations have demonstrated the added value of the improved performance. In the case of orbit maintenance of a geostationary space craft, the new sensors monitor thrust manoeuvres more precisely, allowing autonomous station keeping and reducing the need for ground-based orbit determination.

Measurements and testing were a key part of the project with significant time spent on the definition of specifications and a complete testing plan. Testing equipment was designed and fabricated. Various measurement campaigns were performed demonstrating the preliminary performance of the MEMS devices. Measurements conducted at a low-vibration environment, showed noise levels of 20 ng/√Hz. Allan variance analysis of the same data demonstrated 0.1 μg stability over a significant measurement bandwidth. Results of bias measurements at various temperatures revealed an expected amount of temperature sensitivity. A preliminary thermal residual was estimated though thermal optimization is yet to be done. A summary of all the measured specifications are given in Table 1. Future activities will dive deeper into the performance analysis of the accelerometers and include elements such as shock and radiation tolerance.

Table 1: Summary of target specifications and their preliminary measured values

Parameter	**Target / specification**	**Measured value**
Input range	0.2 – 2 g	0.2 g
Bias stability	< 0.1 µg	0.02 – 0.5 µg
Bias thermal sensitivity	< 100 µg/K	55 µg/K
Bias thermal sensitivity residual	< 10 µg	~ 50 µg (1σ)
Scale factor error	< 80 ppm	< 100 ppm
Velocity random walk	10 – 40 ng/√Hz	20 ng/√Hz
Bias instability (flicker)	14 – 56 ng	28 ng
Bias random walk	190 – 760 ng/√hr	950 ng/√hr
In-band noise: (0 -10 Hz)	42 – 170 ng_{rms}	125 ng_{rms}
(10 – 100 Hz)	95 – 400 ng_{rms}	190 ng_{rms}

The collaboration is excited about the prospect of bringing these novel sensors to the market. This project has set a framework from which further development, testing and validation can be built. It has brought together powerful new sensor technology and world leading experts at ESA to demonstrate to the wider aerospace community what the future of inertial sensing may offer.